Experimental Cyclic Test of Reduced Damage Detailed Drywall Partition Walls Integrated with a Timber Rocking Wall

Hamed Hasani & Keri L. Ryan

Taylor & Francis
Taylor & Francis Group

Check for updates

Experimental Cyclic Test of Reduced Damage Detailed Drywall Partition Walls Integrated with a Timber Rocking Wall

Hamed Hasani (ID) and Keri L. Ryan (ID)

Civil and Environmental Engineering, University of Nevada Reno, Reno, United States

ABSTRACT

Bidirectional quasi-static cyclic loading was applied to a subassembly of drywall partition walls integrated with cross-laminated timber rocking walls. Details aimed to reduce seismic damage to the partition walls were investigated, such as slip connections of partition walls to the diaphragm and gap detailing for the wall intersections. Telescoping detailing eliminated damage to the framing at the wall ends compared to traditional slip-track detailing. The distributed gap wall delayed the damage to about 1% inter-story drift. In the corner gap wall, the sacrificial corner bead opened up at low drifts (0.43%), but the wall was damage-free until more than a 2% drift.

1. Introduction

Modern seismic design methodologies are evolving to focus on the overall building performance rather than strength alone. As such, performance-based design approaches are increasingly used by different design codes (ASCE (American Society of Civil Engineers) 2007; FEMA 2000), which allow a level of seismic protection from immediate occupancy (resilience against natural hazards) to collapse prevention. Whole building resilience requires not only the resilience of the structural system but also the resilience of its non-structural systems. In recent earthquakes, the damage to non-structural components has dominated economic losses, as these components comprise the majority of the construction cost and sustain more frequent damage – leading to subsequent downtime – than structural components (Taghavi and Miranda 2003). In general, the economic loss caused by damaged non-structural components alone, the loss of inventory, and the subsequent business downtime may exceed the replacement cost of the building (Villaverde 1997).

A developing approach that has the potential to offer seismic resilience for timber buildings is the use of post-tensioned cross-laminated timber (CLT) rocking walls as the lateral load resisting system (Buchanan et al. 2008; Ganey 2015). Since rocking wall systems lead to larger inter-story drifts compared to traditional shear walls (Zhou, Li, and Lu 2012), special attention should be given to drift sensitive non-structural components. Only one system-level test on a timber building incorporated a CLT rocking wall system (Pei et al. 2019). In this test, drift ratios of 1.59% to 2.40% were observed for the design earthquake.

Another aspect of rocking wall systems is the vertical displacement incompatibility between the wall and floor diaphragms. When a rocking wall is subject to lateral load, a portion of the wall uplifts as the bottom of the wall rocks up off the base on one side. This uplift causes a rotation and a vertical displacement incompatibility between the wall and the floor at the location of the wall-to-floor connections. While uplift/rotation is not unique to the rocking wall system, in a traditional wall, rotation is distributed along the plastic hinge length, while in a rocking wall, the rotation is concentrated at the base

---

CONTACT Hamed Hasani ✉ hasani@nevada.unr.edu 🖳 Civil and Environmental Engineering, University of Nevada Reno, 1664 N Virginia St, Reno, 89557-0705, United States.

joint. This inconsistency has a significant effect on the performance of non-structural components due to the localized diaphragm displacement at the wall-to-floor connection locations.

In general, different wall-to-floor connections can be used, including rigid connections, connections that allow relative rotation, and connections that allow both relative rotation and vertical movement between the floor and the wall. Moroder et al. (2014) investigated several connections for timber rocking walls and their effect on the diaphragm deformation. They showed that a pin-round hole connection could eliminate rotational incompatibility, which minimizes the system strength increase due to connection resistance. A pin-slotted hole connection was used to allow relative vertical movement, but the joint did not move properly because of friction. A connection with an eccentric group of bolts was found to induce higher rotation and uplift in the beam compared to a centered bolt group connection. In shake-table tests that investigated the experimental behavior of building systems with precast concrete rocking walls (Schoettler et al. 2009) and CLT rocking walls (Pei et al. 2019), special slotted connections successfully isolated the floors from the wall uplift to minimize the localized deflection in the diaphragm. However, there is minimal research on how the lessened local diaphragm deformation affects non-structural components.

Drywall partition walls are among the most common non-structural components in building construction and could considerably affect the seismic resilience of buildings. These components are drift sensitive (ASCE (American Society of Civil Engineers) 2003) and are susceptible to damage at low shaking intensities. Although wood-framed partition walls have higher ultimate capacity compared to steel-framed partition walls (Memari et al. 2008), steel-framed partition walls tend to respond in a more ductile manner (Tasligedik, Pampanin, and Palermo 2012). Therefore, many researchers have investigated the seismic response of steel-framed drywall partition walls, referred to hereafter as partition walls (Hasani et al. 2018, Ryan and Hasani 2020). In particular, local connections in partition walls have been tested under monotonic or cyclic loading. Furthermore, component tests of partition walls in isolation have been conducted under monotonic, cyclic, and dynamic loading protocols. System-level shake table tests have been conducted to evaluate the interaction between partition walls, structural systems, and other non-structural components such as ceilings and facades.

Table 1 summarizes prior experimental studies on partition walls, grouped into local tests, component tests, and system-level tests. Table 1 also lists the type of loading, whether the study developed damages states (DS) and fragility functions, and the construction parameters evaluated. These research projects have pursued a variety of objectives and achieved various outcomes, such as:

(1) *Effect of construction details on seismic behavior of partition walls*: Construction details have a fundamental role in the response of partition walls, as even walls built with the same materials and general construction techniques can exhibit different seismic behavior (Retamales et al. 2013). Some of the studied details are as follows: connection detail of wall to the surrounding elements horizontally (CWH) or vertically (CWV); wall discontinuities (WD) such as door frame and window; partial height drywall (PHD); drywall screw (DS), track to diaphragm screw (TDS), and stud to track screw (STS) spacing and layout; drywall placement (DP) details including dimension, thickness, and type of drywall panels; vertical slotted track (VS); framing properties (FP) such as stud/track gage, size, spacing and material (steel or wood); wall intersection (WI); the gap between stud and track (GST); joint finishing details (JF); wall aspect ratio (AR); partial height walls (PHW); blocking (BE); and reduced damage details in the wall (RDD).

(2) *Definition of damage states and fragility curves*: A few researchers studied damage data to develop damage state definitions and seismic fragilities, such as Rihal (1982), who was a pioneer in this area. The probability of occurrence of a given damage state is usually expressed as a fragility curve function associated with an inter-story drift ratio since the partition walls are drift-sensitive components. Some of the research data has been used for defining general fragility functions for partition walls as part of the FEMA *P*-58 project (Mosqueda 2016).

Table 1. Prior studies of partition walls.

	Authors	Type of test – direction	DS	Construction parameter
Local Tests	(Swensen, Deierlein, and Miranda 2015)	monotonic and cyclic – quasi-static – X		DS
	(Rahmanishamsi, Soroushian, and Maragakis 2016b)	monotonic and cyclic – quasi-static – X	Yes	DS, FP
	(Rahmanishamsi, Soroushian, and Maragakis 2016a)	monotonic and cyclic – quasi-static – Y	Yes	GST, FP, STS
	(Fiorino et al. 2017)	monotonic and cyclic – quasi-static – X		DS, DP
Component Test	(John A. Blume 1966)	cyclic – quasi-static – X	Yes	CWH, WD, FP, DP
	(John A. Blume 1968)	cyclic – quasi-static – X	Yes	CWH, WD, FP, DP
	Freeman 1971	cyclic – quasi-static and dynamic – X	Yes	CWH, WD, FP, DP, DS, BE
	Freeman 1974	cyclic – quasi-static and dynamic – X	Yes	CWH, FP, DP, WI, DS, BE
	Freeman 1976	cyclic – quasi-static – X	Yes	CWH, FP, DP
	Rihal 1982	cyclic – quasi-static – X	Yes	CWH, WD, PHD, DS, DP, FP, GST, JF
	Lee et al. 2007	cyclic – quasi-static and dynamic – X		WD, WI
	Memari et al. 2008	monotonic and cyclic – quasi-static – X		FP, JF
	Restrepo and Lang 2011	cyclic – quasi-static – X + Y	Yes	
	Restrepo and Bersofsky 2011	cyclic – quasi-static – X	Yes	WD, PHD, DS, DP, VS, FP, WI
	Peck, Rogers, and Serrette 2012	monotonic and cyclic – quasi-static – X		DS, DP, FP, AR, BE
	Tasligedik, Pampanin, and Palermo 2012	cyclic – quasi-static – X		FP
	Retamales et al. 2013	UB-NCS – X, Y	Yes	CWH, DS, FP, WI, PHW, RDD
	Tasligedik, Pampanin, and Palermo 2013	cyclic – quasi-static – X		FP, RDD
	Magliulo et al. 2014	shake sable – X + Y	Yes	
	Petrone et al. 2015	cyclic – quasi-static – X	Yes	DS, DP, FP
	Petrone et al. 2016	cyclic – quasi-static – Y		FP, DP
	Pali et al. 2018	cyclic – quasi-static – X	Yes	CWH, CWV, DP, FP, JF
	Fiorino, Pali, and Landolfo 2018	monotonic – quasi-static and dynamic- Y		CWH, AR, FP, TDS
	Araya-Letelier, Miranda, and Deierlein 2019	cyclic – quasi-static – X		CWH, RDD
System-Level Test	Matsuoka et al. 2008	shake table – X + Y	Yes	RDD
	McCormick et al. 2008	shake table – X	Yes	
	Retamales et al. 2011	UB-NCS – X		
	Wang et al. 2015	shake table – X	Yes	
	Soroushian et al. 2012	shake table – X + Y, X + Y + Z		CWH, WD, FP, WI
	Jenkins et al. 2016	shake table – X + Y	Yes	CWH, WD, FP, WI, PHW, RDD
	Fiorino, Bucciero, and Landolfo 2019	shake table – X	Yes	CWH, CWV

(3) *Estimation of repair cost*: Lee et al. (2007) found that partition wall repair was not required for drift levels below 0.25%. At drift levels of 2%, the repair cost of partition walls equaled their initial construction cost, while at drift levels of 8%, repair costs were twice the initial construction costs. Araya-Letelier and Miranda (2012) showed that the expected annual loss of conventional partition walls is eight times larger than the annual loss of partition walls incorporating novel sliding/frictional connections, and even more if the environmental impact is considered. In another study, the partition wall repair costs were estimated to be up to the initial cost for the serviceability damage state, and up to twice the initial cost for damage beyond serviceability level (Fiorino, Bucciero, and Landolfo 2019; Pali et al. 2018).

(4) *Effect of loading protocol*: The number of cycles had only limited effects on the seismic performance of partition wall specimens tested with quasi-static loading (Restrepo and Lang 2011). Based on that, FEMA 461 (Applied Technology Council 2007), which developed interim loading protocols for seismic qualification tests of components, investigated two loading protocols and found that step increment does not considerably affect the response. Furthermore, partition wall

damage was not found to be amplified by dynamic loading compared to quasi-static loading (Lee et al. 2007), and a monotonic test was recommended as a reasonable estimate for the envelope of a cyclic test (Memari et al. 2008; Peck, Rogers, and Serrette 2012). Fiorino, Bucciero, and Landolfo (2019) found that partition walls sustained no damage when subjected to out-of-plane seismic loading alone. However, the literature lacks a systematic comparison of in-plane and bidirectional loading of partition walls for understanding the effect of out of plane loading on in-plane resistance.

(5) *Contribution of non-structural components in structural response*: A few researchers examined the contribution of partition walls to the lateral resistance of the structure. In quasi-static tests, the strength of partition walls was shown to be non-negligible compared to the structure when tested as an infill wall in an enclosed frame of beams and columns, whether using slip-track detailing (Lee et al. 2007) or fixed connections (Tasligedik, Pampanin, and Palermo 2012). Also, the influence of partition walls on dynamic properties of buildings was investigated with some dynamic tests on a shake table by measuring secant stiffness, damping, and the fundamental frequency of the building (Fiorino, Bucciero, and Landolfo 2019; Magliulo et al. 2014; Matsuoka et al. 2008; McCormick et al. 2008; Soroushian et al. 2016; Wang et al. 2015). Due to the inherent flexibility of CLT rocking walls, partition walls could contribute significantly to the overall resistance of the building.

While many details have been studied (Table 1), the construction details found to most affect the partition wall seismic response are the connection details of the walls to the surrounding elements (Pali et al. 2018). In general, there are two approaches for connecting partition walls to the surrounding structural elements: "fixed" and "slip-track" connections. In fixed detailing, the studs and drywall are connected to tracks on top and bottom. In slip-track detailing, the partition walls are isolated from the inter-story drift by eliminating the connection of studs and drywall to the top track. The slip-track connections reduced damage associated with drift but increased damage at the wall-intersections compared to fixed connections. The slip-track connections were also associated with damage from studs popping out of tracks at the wall ends (Retamales et al. 2013). Moreover, the presence of intersecting walls in slip-track detailing with the slip detail on top and bottom caused partition walls to sustain rocking during in-plane motion (McCormick et al. 2008).

In this study, to expand the knowledge of the seismic response of partition walls, two sets of partition walls with innovative details aimed at reducing drift-induced damage were experimentally evaluated using a bidirectional loading protocol. In both phases, partition walls were built within a post-tensioned CLT rocking wall subassembly. The objectives of this study are to evaluate the effect of out-of-plane drift on the partition wall in-plane resisting force, to evaluate the contribution of the partition walls to the overall structural strength and stiffness, and to evaluate the effectiveness of the innovative construction details on damage states. In Phase 1, a telescoping (track-within-a-track) deflection assembly is compared to conventional slip-track detailing in straight walls. Both details permit sliding of the top of the wall relative to the diaphragm, but the telescoping detailing, which has been used mainly for absorbing the vertical deflection of the diaphragm, has not – to the authors' knowledge – been tested under lateral loading (Applied Technology Council 2012). In Phase 2, two C-shaped walls with details aimed at reducing damage at wall intersections are evaluated. The distributed gap (DG) detail incorporates more frequent expansion joints through the length of the wall to absorb some of the in-plane movement and delay the collision with the intersecting wall. The corner gap (CG) detail incorporates a full gap through the wall intersection to allow intersecting walls to penetrate the corner region without damage. The CG detailing has been proven to reduce damage at the wall-intersection for in-plane loading, but the performance under bidirectional loading has not been investigated (Retamales et al. 2013).

2. Test Program

As mentioned above, the experimental program consisted of bidirectional tests on full-scale partition walls constructed within a post-tensioned CLT rocking wall subassembly at the Natural Hazard Engineering Research Infrastructure (NHERI) Lehigh Equipment Facility (EF). This testing was conducted as part of the NSF collaborative NHERI TallWood Research Program (NHERI TallWood-Home 2020). The partition wall configurations integrated within the CLT rocking wall subassembly are illustrated in Fig. 1. In particular, Phase 1 consisted of two straight partition walls (Fig. 1(a)), and Phase 2 consisted of two C-shaped wall assemblies (Fig. 1(b)).

2.1. Test-bed Setup

The structural test-bed specimen, designed by Lehigh University (Bond et al. 2018; Clay et al. 2019), was a post-tensioned CLT rocking wall subassembly. The test-bed was used to impose bidirectional cyclic loading on partition walls installed between the CLT base and floor diaphragms. Figure 2(a)
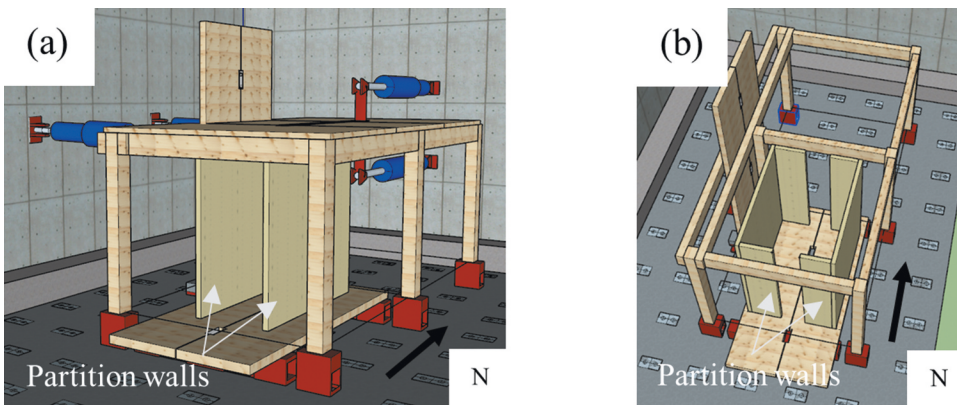

Figure 1. Configurations of partition walls: (a) Phase 1, (b) Phase 2.
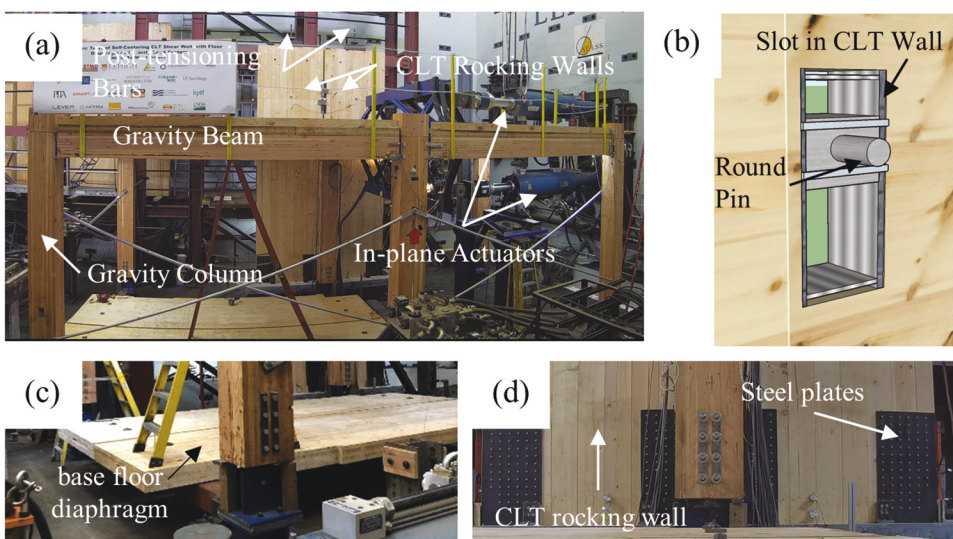

Figure 2. Structural test specimen; (a) test specimen, (b) collector-beam-to-CLT rocking wall connection, (c) base floor diaphragm, (d) repaired CLT rocking wall.

shows the different parts of the test-bed specimen. U-shaped flexural plates connected coupled post-tensioned CLT rocking walls for energy dissipation. Each wall was constructed from a 5-layer (175 mm thick) Spruce-Pine-Fir South (SPF-S) CLT panel with dimensions 1.52 m long by 6.1 m high, and was post-tensioned with an 806 mm^2 steel to the foundation at the center of the panel to produce a self-centering response. Two 222 mm x 419 mm Douglas-Fir (DF) glulam collector beams were connected to the CLT rocking wall from both sides to deliver the lateral forces from the 3-layer SPF-S CLT floor diaphragm to the CLT rocking wall. The collector beam to the CLT rocking wall connection was a round pin through a vertical slot at the wall (Fig. 2(b)). The connection was designed so that the collector beam and floor diaphragm do not uplift when the CLT rocking wall rocks up off the foundation. Out-of-plane rubber bearings, sliding on a Teflon surface, were designed to transfer the out-of-plane loading from the floor diaphragm to the CLT rocking wall and to brace the CLT rocking wall in the out-of-plane direction. The gravity load system consisted of 140 mm x 305 mm DF glulam beams and 311 mm x 381 mm DF glulam columns with pinned bases. The base diaphragm consisted of two separate five-ply CLT panels placed on friction Teflon pads, which allowed the forces in each partition wall to be measured by axial load cells (Fig. 2(c)).

The partition wall tests followed a series of tests on the structural test-bed performed by Lehigh University. Prior to the partition wall tests, the CLT rocking walls were repaired (Fig. 2(d)) by attaching steel plates with wood screws to the corner of each wall panel.

2.2. Test-specimen Detail

Partition wall dimensions are illustrated in Fig. 3. The partition walls for Phase 1 were 3.69 m long (Fig. 3(a)). For Phase 2, the clear lengths of the walls between return walls were 3.45 m for the CG wall and 3.49 m for the DG wall. The return walls (intersecting walls) were 0.92 m long and 0.85 m long respectively (Fig. 3(b)). Discrepancies in wall lengths were due to differences in the gap detailing. All walls were 3.81 m high.

The partition walls adopted in both phases were built according to common construction practice for institutional slip track detailing, and the wall design was checked against out-of-plane deflection limits for a horizontal load of 0.24 kN/m^2 (IBC 2011; SSMA (Steel Stud Manufacturers Association) 2000a; SSMA (Steel Stud Manufacturers Association) 2000b). Figure 4(a) illustrates the partition wall components, and Table 2 lists the framing and material specifications for the partition walls. The walls were framed from steel with a nominal minimum yield strength of 227.53 MPa, and the studs were spaced at 406 mm o.c. The framing was sheathed with a 15.9 mm thick standard drywall. Self-drill screws were used for all stud-to-track connections (4.8 mm diameter screws) and drywall-to-stud connections (3.5 and 4.2 mm diameter screws). The studs and drywall were generally fixed to the bottom tracks (Fig. 4(b)). Corner-bead sticks with 35.1 mm legs were generally used for outside corners. All walls were taped and painted according to standard finishing procedures.

Figure 5 shows the proposed details for damage reduction considered in this study. As mentioned previously, two details for connecting the partition wall to the floor diaphragm were considered in Phase 1: slip-track detailing (Fig. 5(a)) and telescoping detailing (Fig. 5(b)). In the slip-track detailing,
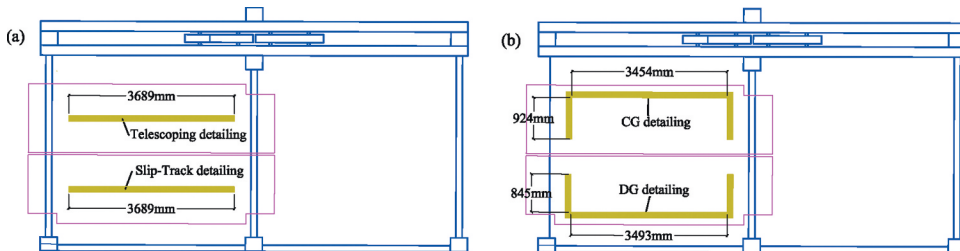

Figure 3. Placement of walls in the test-bed structure and dimension of walls; (a) Phase 1, (b) Phase 2.
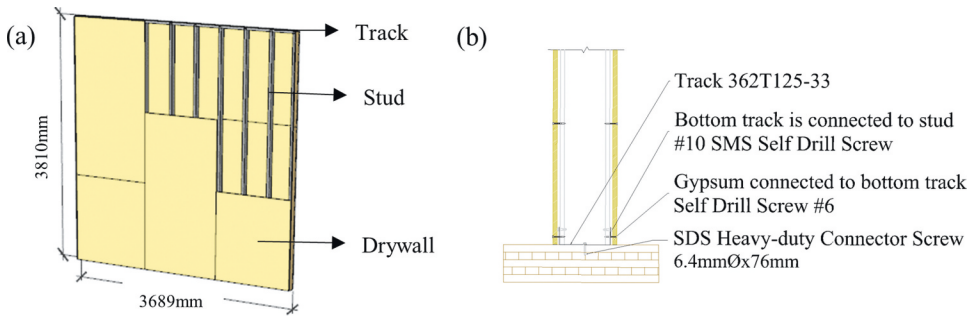
Figure 4. (a) Partition walls components – 3D view, (b) detail of connection of walls to the bottom diaphragm.

Table 2. Nominal dimensions and material properties of partition walls.

Studs	362S125-33	92.08 mm width x 31.75 mm leg height x 0.84 mm thickness
Tracks	362T125-33	92.08 mm width x 31.75 mm leg height x 0.84 mm thickness
	362T200-33	92.08 mm width x 50.8 mm leg height x 0.84 mm thickness
	362T250-43	92.08 mm width x 63.5 mm leg height x 1.09 mm thickness
	375T200-54	95.25 mm width x 50.8 mm leg height x 1.37 mm thickness
Track to diaphragm screws	SDS Heavy-duty connector screw 6.35 mm Ø x 76.2 mm @ 305 mm, and 152 mm at corner zone	
Frame screws	#10 SMS Self Drill Screw	
Drywall to frame screws	Self-Drill Screw #6 at 203 mm o.c. on boundaries and 305 mm o.c. on the field (#8 for 2 or 3 layers attachments)	
Finishing	Joints	Paper tape attached with plaster-based compound and covered with two coats of plaster-based compound
	Fasteners	Covered with three coats of plaster-based compound
	Expansion joints	PVC "V" expansion joints with the allowable movement of 9.5 mm attached with spray adhesive
	CG angles	Covered with flexible corner bead with a leg width of 57.2 mm
	Exterior angles	Covered with corner-bead sticks with the 35.1 mm legs

the studs and drywall were not connected to the top track, allowing the studs to slip relative to the top track. In telescoping detailing, the sliding occurred between an inner track nested within an outer track, while all the studs and the drywall were connected only to the inner track.

Phase 2 incorporated the DG detailing and CG detailing into conventional slip-track walls to reduce damage at the wall-intersections. Expansion joints are usually limited to the mid-wall region, but in the DG detailing tested here, expansion joints were also located adjacent to the return walls. Both non-fire-rated (Fig. 5(c),Fig. 5(d)) and fire-rated (Fig. 5(e),Fig. 5(f)) expansion joints were incorporated adjacent to the wall intersection and in the wall interior, respectively. In the fire-rated expansion joints, two layers of drywall were added within the joint to prevent fire intrusion. PVC "V" expansion joints with an allowable movement of 9.5 mm were attached with spray adhesive. The drywall was not screwed at the bottom of the DG wall to provide a hinge connection and better accommodate the movement permitted by the expansion joints.

In the CG wall, tracks and studs were not extended into the corner region, to allow slip movement of the walls to penetrate the intersection (Fig. 5(g)). The corner region was filled with mineral wool for fire protection. Moreover, the angles of the CG wall were covered with a flexible corner bead with a leg width of 57.2 mm.

2.3. Loading Protocol and Instrumentation

Photos of relevant instrumentation for the structural specimen are shown in Fig. 6. Plastic slides at the bottom of the CLT rocking wall measured its uplift, and string pots connected to the collector beam (only attached in Phase 2) measured its vertical movement (Fig. 6(a)). Load cells attached at the end of
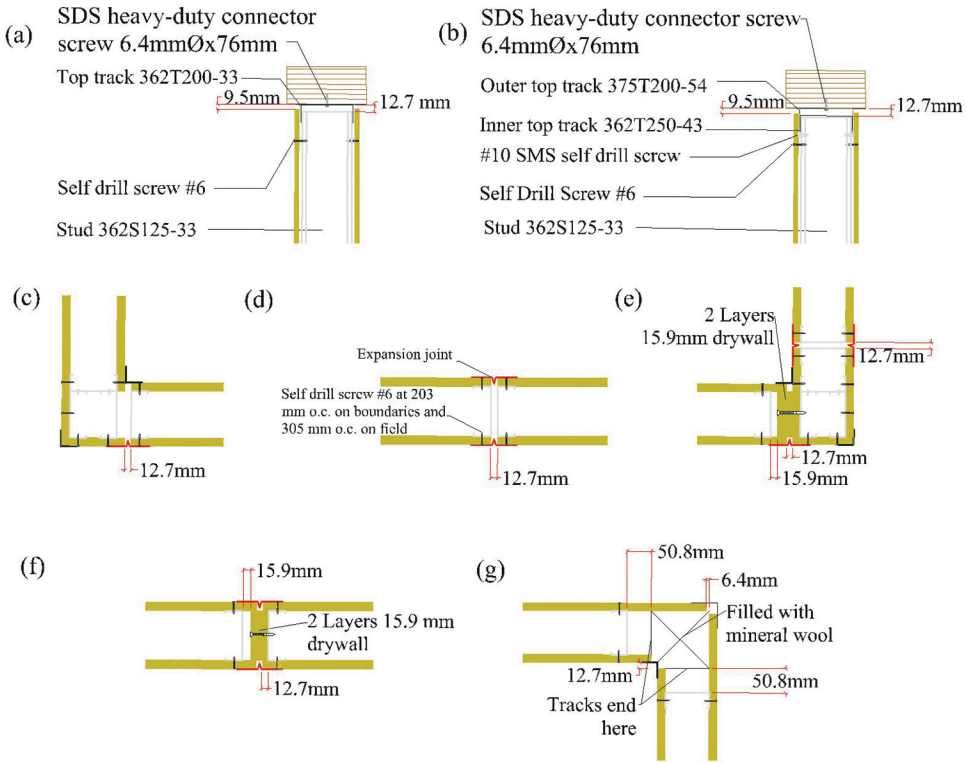
Figure 5. Details adopted in phases 1 and 2 for damage reduction; (a) slip-track connection, (b) telescoping connection, (c) wall intersection non-fire-rated expansion joint, (d) interior non-fire-rated expansion joint, (e) wall intersection fire-rated expansion joint, (f) Interior fire-rated expansion joint, (g) corner gap detail.
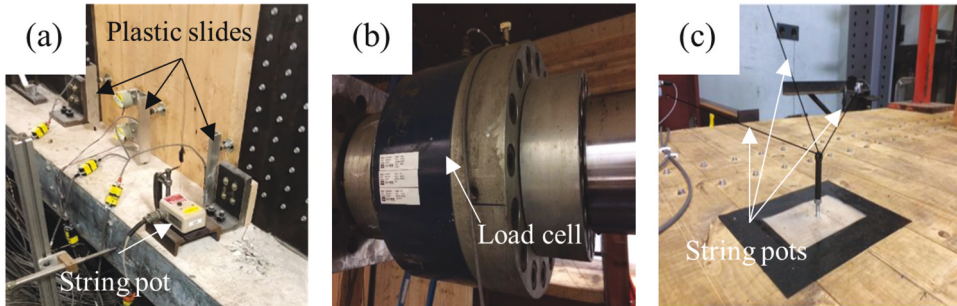

Figure 6. Instruments on the structural specimen; (a) string pot and plastic slide to measure uplift in collector beam and wall, (b) load cells on actuators to measure the force in the building, (c) string pot connected to the SPN.

each actuator measured the total lateral force in the subassembly (Fig. 6(b)). String potentiometers measured the structure-physical node (SPN) displacement (Fig. 6(c)).

The layouts of the partition wall instrumentation for Phases 1 and 2 are provided in Fig. 7(a,Fig. 7(b)), respectively, while pictures of instrumentation are shown in Fig. 8. Figure 8(a) shows plastic slides that measure the slip of the bottom track and rocking of walls in Phase 1 (PSE1, PSE5, PSE4, PSE8, PSW1, PSW5, PSW4 and PSW8 in Fig. 7(a)). Figure 8(b) shows a unidirectional load cell attached to the bottom diaphragm. Figure 8(c) shows an example of a plastic slide used to measure the vertical gap at the top of the walls (PSW2, PSW3, PSE2 and PSE3 in Fig. 7(a), and PSW1, PSW4, PSW5, PSW8, PSE1, PSE4,
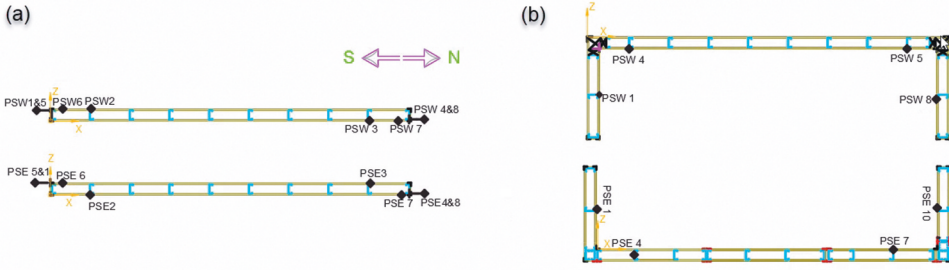
Figure 7. Schematic view with the indication of the adopted instrumentations; (a) Phase 1, (b) Phase 2.
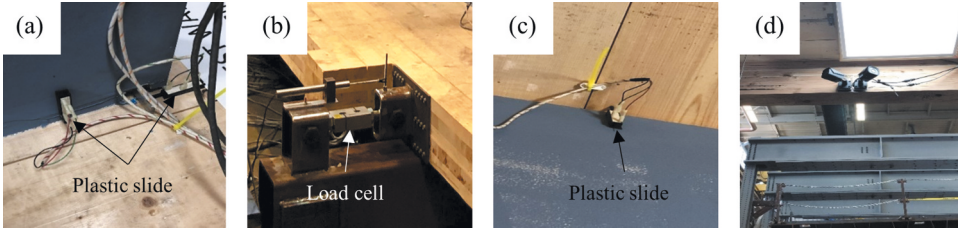

Figure 8. Instrumentation; (a) plastic slides for measuring track slide and rocking of partition wall, (b) load cell for measuring the force in the partition wall, (c) plastic slide for measuring gap at the top of the wall, (d) cameras.

PSW7, and PSE10 in Fig. 7(b)). Figure 8(d) shows the cameras that are used for continuously following the damage, and some of the videos are available online (NHERI TallWood Research Tasks 2020).

The test specimen was subjected to displacement-controlled bidirectional loading imposed by actuators connected to the CLT floor diaphragm of the subassembly. Loading in the direction of the lateral load resisting system (in-plane) was applied by two in-plane actuators and in the out-of-plane direction by two out-of-plane actuators. The movement of the test subassembly was controlled by the SPN, wherein displacement commands were imposed through a relationship between the SPN and the actuators.

A cyclic drift loading protocol was used for this test. The loading protocol specified a bidirectional path of movement, with three sub-cycles in each stage: in-plane, bidirectional hexagonal, and bidirectional hexagonal with an increase in out-of-plane drift (Fig. 9(a)). The magnitude of peak in-plane drift was increased in each stage, as shown in Fig. 9(b). The Phase 1 walls were loaded to 5% drift and the Phase 2 walls to 4% drift. This loading protocol was designed to evaluate the effect of the out-of-plane drift on the in-plane resistance of the partition wall. The loading protocol was based on FEMA 461 (Applied Technology Council 2007) but with additional cycles in each stage. After the first two
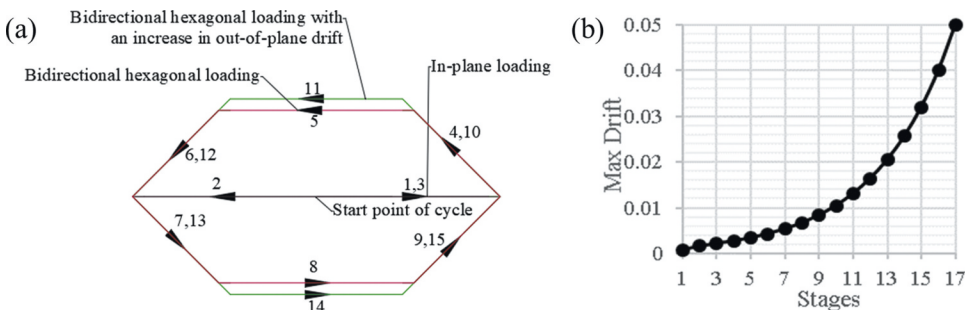

Figure 9. (a) Path of movement of the bidirectional load step, (b) peak in-plane drift amplitude in different stages.

Table 3. Loading protocol.

Stage	In-plane Wall Drift at Floor Level % (mm)	Out-of-plane plane Wall Drift at Floor Level % (mm)	Cycles	Loading Rate (mm/min)
A	0.08 (3)	0.04 (2)	3	15
B	0.16 (6)	0.08 (3)	3	15
C	0.22 (8)	0.11 (4)	1	15
D	0.27 (10)	0.14 (5)	1	20
E	0.34 (13)	0.17 (7)	1	20
F	0.43 (16)	0.21 (8)	1	20
G	0.54 (21)	0.27 (11)	1	20
H	0.67 (26)	0.33 (13)	1	30
I	0.84 (32)	0.42 (16)	1	30
J	1.05 (40)	0.52 (20)	1	30
K	1.31 (50)	0.65 (25)	1	30
L	1.64 (57)	0.82 (29)	1	30
M	2.05 (78)	1.02 (39)	1	35
N	2.56 (98)	1.28 (49)	1	35
O	3.2 (122)	1.6 (61)	1	35
P	4 (152)	2 (76)	1	40
Q	5 (191)	2.5 (96)	1	40

stages, the amplitude was increased by a factor of 1.25 in each stage. These modifications were introduced to capture the wall damage for both minimal and high drift ratios. Table 3 shows the drift, displacement, and loading rate of each cycle. The displacement-controlled test procedure varied the displacement rate between 15 to 40 mm/min (Table 3). The data were recorded with a sampling frequency of 8 Hz.

3. Test Results

3.1. Damage Observations

The seismic performance of the partition walls was evaluated through observation of the damage mechanisms. The primary damage measures observed in the partition wall specimens in both phases are shown in Fig. 10. In this figure, T refers to telescoping detailed, and ST refers to slip-track detailed Phase 1 walls, while CG refers to the corner gap, and DG refers to distributed gap Phase 2 walls. In Figure 10, Images 1 and Images 2, respectively, depict detachment of the corner bead and warping of the drywall, which were observed in both the slip-track and telescoping walls when the track leg pushed against the end drywall. Images 3–5 depict the opening of the corner bead, bending of the end stud, and bending of the track leg, which were all observed only in the slip-track wall. These occurrences corresponded to a significant increase in the resisting force of the wall when the end stud passed the end of the track and could not slide back into place upon cyclic reversal.

At a drift of 0.43%, the sacrificial corner beads detached from the CG wall due to the incompatible movement of in-plane and out-of-plane drywall (Image 6). Damage to the track leg in the CG wall (Image 7) was similar to that observed in Image 5. Damage to the end stud (Image 8) and permanent movement of the CG return wall (Image 9) were observed in post-test inspections after the drywall was removed. This damage was believed to have occurred at 78 mm (2.05%) drift after the end stud slid past the end of the track. Note that this drift corresponded to approximately the length of the track beyond the stud (50.8 mm) plus the stud leg length (31.8 mm). The first damage observed in the DG wall was the detachment, or opening of the expansion joint when its limit was reached (Image 10). After the expansion joint closed, the track leg of the return wall opened or bent (Image 11), and the studs of the main wall pushed against the return wall. In Images 12 and 13, the wall completely separated at the expansion joint due to the repeated cyclic opening and closing of the joint, causing extensive damage to the stud and track. The introduction of expansion joints on both walls immediately adjacent to the wall intersection (fire-rated detailing) led to a stability issue because, as both joints opened, a small wall section at the corner detached and became isolated. Post-test inspections of the DG wall after removal of

1. T: Detachment of corner bead (0.43% drift)

2. ST: Warping of drywall (0.67% drift)

3. ST: Opening of corner bead due to bending of stud (0.84% drift)

4. ST: Bending of end stud (2.56% drift)

5. ST: bending of leg of track (3.2% drift)

6. CG: Detachment of corner bead (0.43% drift)

7. CG: Damage to the leg of track (2.56% drift)

8. CG: Damage to end stud (after test)

9. CG. Permanent movement of return wall (after test)

10. DG: Detachment of expansion joint (0.84% drift)

11. DG: Opening of leg of track (1.05% drift)

12. DG: Big opening at expansion joint fire-rated (2.56% drift)

13. DG: Big opening at expansion joint non-fire-rated (after test)

14. DG: Permanent movement of return wall (after test)

15. DG: Damage to the studs and tracks (after test)

Figure 10. Observed damages to partition walls at various stages of testing: T = Telescoping, ST = Slip-track, CG = Corner gap, DG = Distributed gap.

drywall showed the permanent movement of the return wall (Image 14) similar to Image 9 and damage to the studs and tracks (Image 15) due to the impact of the main wall and the return wall.

Figure 11(a,Figure 11(b),Figure 11(c),Figure 11(d)) shows the force versus drift hysteresis loops in each partition wall. The likely occurrences of the damage measures in Figure 10 are indicated on the hysteresis loops with corresponding numbers 1–14. Some damage to the slip track wall (Images 3 and Images 3(5)) occurred during the bidirectional loading, which indicates that bidirectional loading
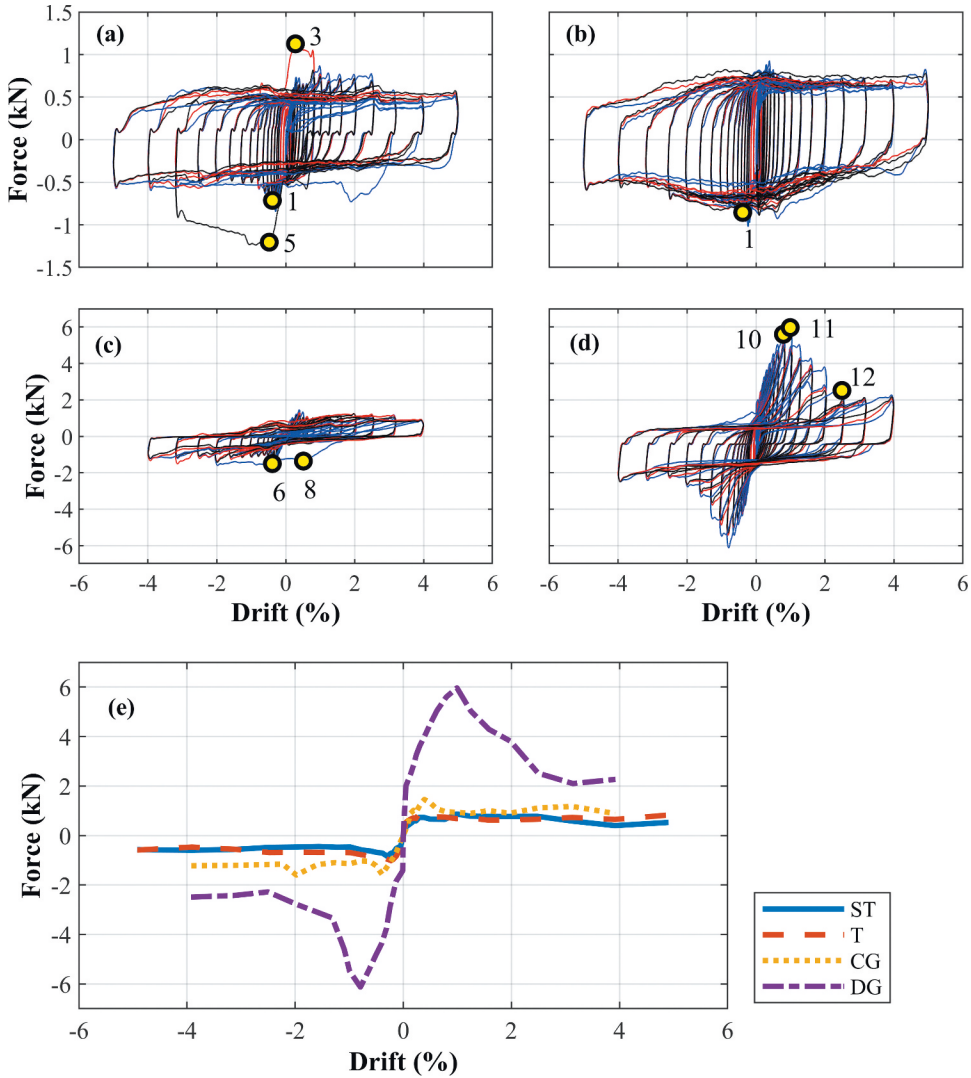
Figure 11. Experimental load versus inter-story drift with an indication of damage progression; (a) slip track, (b) telescoping, (c) corner gap, (d) distributed gap; blue = in-plane cycle, red = bidirectional cycle 1, black = bidirectional cycle 2, (e): backbone curves.

contributed to the initiation of damage. These damage occurrences corresponded to sudden increases in force on the hysteretic loops. Since the slip-track (Fig. 11(a)) and telescoping walls (Fig. 11(b)) have similar slip behavior, the magnitude of forces generated in each wall was similar. Because the CG wall did not have studs and tracks in the wall intersection that allowed the walls to penetrate the intersection, its resisting force was similar to the Phase 1 walls without return walls (Fig. 11(c)). However, the DG wall experienced significant resistance from the collisions at the wall-intersection after the expansion joints closed (Fig. 11(d)). The differences in the response of different walls, including the resistance and stiffness, are summarized in Fig. 11(e), which shows the backbone curves of in-plane cycles of all wall specimens. Although these backbone curves did not capture peaks that occurred during out-of-plane cycles, they are useful for the relative comparison of walls.

For each wall specimen, the strength was evaluated by calculating the average value of the maximum and minimum values of resisting force from the backbone curves (Fig. 12(a)), and the stiffness as the peak-to-peak stiffness between these two points (Fig. 12(b)). The strength and stiffness
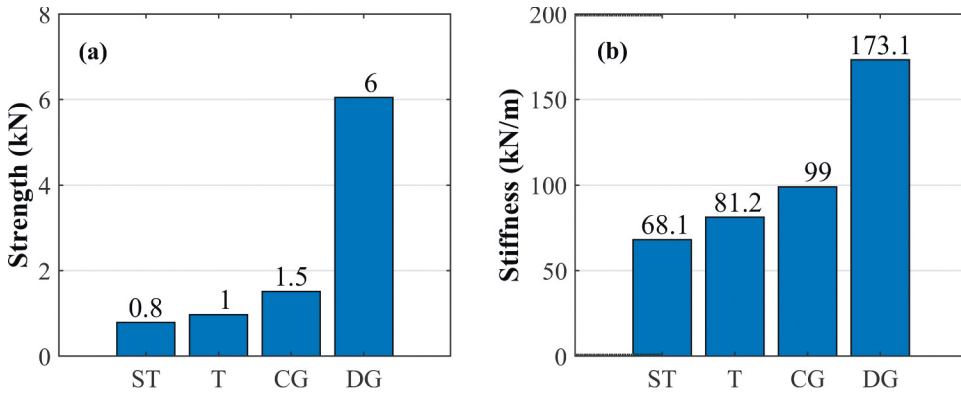
Figure 12. (a) Peak strength and (b) corresponding secant stiffness of each partition wall.

values (0.8 kN and 68.1 kN/m for slip-track compared to 1.0 kN and 81.2 kN/m for telescoping) suggest that even with a similar slip behavior at the top, the friction was slightly higher in the telescoping detailing. The average maximum force that developed in the DG wall was much higher than in the CG wall (6.0 kN compared to 1.5 kN) because the DG detailing led to typical resistance at the intersection walls after the expansion joints closed, while the CG wall responded similarly to the Phase 1 walls without return walls. The difference in the secant stiffness was much less than the difference in the strength (173.1 kN/m for DG compared to 99.0 kN/m for the CG) because of the peak force in the DG wall occurred at a larger drift.

The hysteresis loops of the entire sub-assembly (CLT rocking walls and partition walls) are compared to those of the structural sub-assembly alone in Fig. 13 for both test phases. For Phase 1, there is not a noticeable difference when the resistance of the partition walls is included in the hysteresis loops (Fig. 13(a)). For Phase 2, only a slight difference between the two curves is visible (Fig. 13(b)). Specifically, in Phase 1, the partition walls contributed 0.6% to the whole subassembly
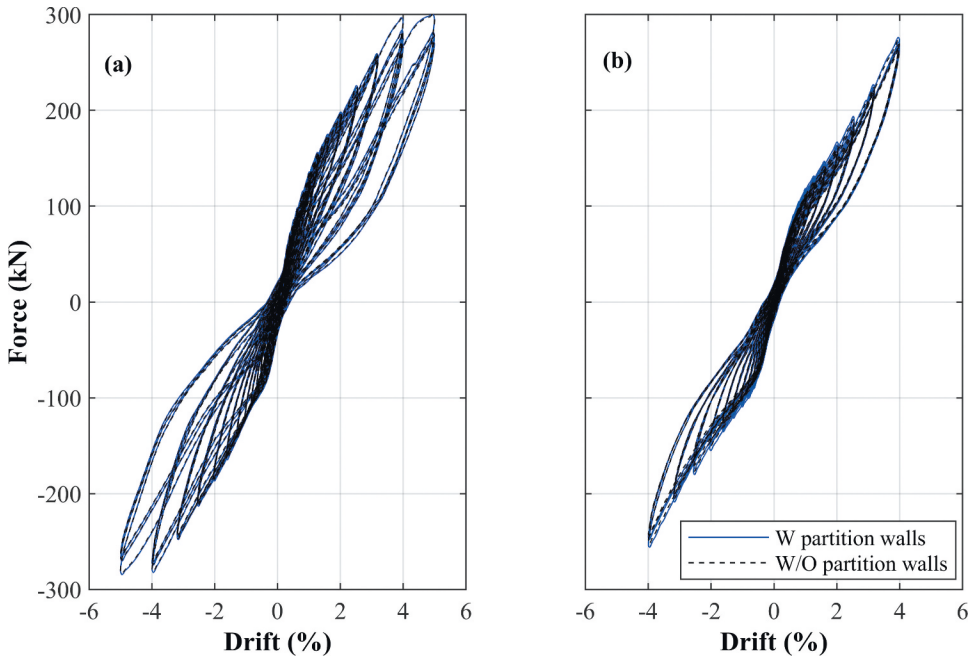

Figure 13. Hysteresis of building in the in-plane direction; (a) Phase 1, (b) Phase 2.

force (1.8 kN of 292.8 kN) and 10% to the whole subassembly stiffness (149.3 kN/m of 1516.9 kN/m). In Phase 2, the partition walls contributed less than 3% to the total force (7.5 kN of 266.1 kN) and about 16% to the stiffness (272.1 kN/m of 1719.4 kN/m) of the whole subassembly. The resistance of partition walls in Phase 2 increased due to the impeding effect of the return walls, but their contribution to the subassembly resistance was still minor. Note that the peak forces in the partition walls occurred at low drifts (average of 1.2%), but the peak force of the subassembly was observed at the peak drifts. Therefore, the partition walls contribute more significantly to the initial resistance than to the limit state responses.

Even after repairs were made to the CLT panels of the rocking walls, there was still stiffness degradation due to localized bearing, spalling of the concrete footings at the corners, and deformation in the connection between the steel plates and the CLT wall panels. Thus, assuming the lateral system is initially undamaged, the resistance of the partition walls likely need not be accounted for in the lateral system design for a large earthquake. However, the numbers provided here could be used to estimate the inter-story stiffness and strength contributions of partition walls based on total wall length in each direction.

3.2. Correlation between Damage Limit States and Drifts

Next, the damage observations in these tests are correlated to standard damage states characterized by damage observation class and, most importantly, required repair actions. Based on the FEMA-P58 background document for partition walls (Mosqueda 2016), in Damage State 1 (DS 1), the wall needs minor drywall patching, taping, and painting. InDS 2, wall needs more drywall patching, taping and painting, and replacement of a few boundary studs. In DS 3, at least half of the wall requires replacement, and the whole wall requires repainting. Table 4 also presents the drift ratio at which each damage state was observed in each test specimen. For some walls, multiple damage observations can be interpreted as DS 3, but for evaluation purposes, the first observation (minimum drift) corresponding to a defined DS was selected. Furthermore, Tables 5 and Tables 6 compare drift ratios corresponding to partition wall DSs for Phase 1 and Phase 2 walls, respectively, to other prior experimental studies of similarly configured walls. Prior studies in Table 5 are restricted to institutional slip-track detailing, with a similar stud to bottom track connections as the Phase 1 walls here. Note that while efforts have been made to be consistent, discrepancies in DS drifts may occur due to different loading protocols, experimental setup, detailing, or even interpretation of the DS definition.

Besides the two Phase 1 walls, two other studies evaluated institutional slip-track detailing without return walls: Davies et al.(2011) and Jenkins et al. (2016). The telescoping detail examined in this study

Table 4. Inter-story drift ratio (IDR) levels recorded at different damage states.

DSs and Damage Phenomena		ST(%)	T(%)	CG(%)	DG(%)
DS1	Medium/severe opening of corner bead	0.43	0.43	0.43	0.84
DS2	Bending of end stud	0.84	-	2.05	1.05
DS3	Bending of the leg of the track	3.20	-	2.56	1.05
	Large opening at expansion joint	-	-	-	2.56
	Permanent movement of the return wall	-	-	4.00	4.00

Table 5. Comparison of drift ratios for straight walls (no return walls) with institutional slip track detailing.

Damage state	DS1 (%)	DS2 (%)	DS3 (%)
(Davies et al. 2011)	0.53	0.81	1.66
(Jenkins et al. 2016)	2.07	2.07	-
Phase 1-ST	0.43	0.84	3.2
Phase 1-T	0.43	-	-

Table 6. Comparison of drift ratios for intersecting walls with various low damage detailing.

Damage state	DS 1 (%)	DS 2 (%)	DS 3 (%)
(Mosqueda 2016)	0.4	1.1	1.9
(Araya-Letelier, Miranda, and Deierlein 2019)	1.5–2.1	1.5–2.1	3
(Retamales et al. 2013)-CG	0.6	-	-
(Retamales et al. 2013)-DST	1.00	1.35	1.84
Phase 2-CG	0.43	2.05	2.56
Phase 2-DG	0.84	1.05	1.05

(Phase 1-T) was observed to eliminate damage to the framing of partition walls caused by the separation of the end studs from the track at large drifts that occurred in the other walls (Table 5). Thus, DS 2 and beyond were never observed in the Phase 1-T wall, while studies of traditional slip track detailing observed DS 2 at drifts ranging from 0.81%-2.07%. DS 1 and DS 2 were observed at larger drifts in Jenkins et al. (2016) compared to the Phase 1-ST wall; the reason is unclear, but perhaps these wall ends were better detailed to avoid damage during sliding, and only the Phase 1-ST wall was subjected to bidirectional loading. DS3 was not observed in one of the specimens in Davies et al. (2011), but it was observed in the two other specimen with an average of 1.66%.

Table 6 focuses on reduced damage detailing for wall intersections and is restricted to C-shaped/T-shaped walls with return walls. Besides the Phase 2 CG and DG walls, studies included in Table 6 are Mosqueda (2016), Retamales et al. (2013), and Araya-Letelier, Miranda, and Deierlein (2019). Mosqueda (2016) represents the average based on fragility functions for typical slip track detailing. Retamales et al. (2013) tested a CG detailing similar to the Phase 2 CG wall, and a double slip-track detailing. In double slip-track (DST) detailing, nail fasteners of the top and bottom track to the slabs are eliminated within 1200 mm of intersecting walls, and the out-of-plane flexibility of the transverse walls is relied on to reduce the contact forces. Araya-Letelier, Miranda, and Deierlein (2019) evaluated a different detail to allow the partition wall to slip relative to the diaphragm above called the "sliding/frictional connection." In this connection, the upper track is placed between a thin plate connected to the upper slab and a short square or rectangular steel tube. The upper track has 88.9 mm circular holes centered around anchors that clamp the tube to the slab above. The clamping force is specified to control the friction, and the holes allow movement in both directions so that intersecting walls can move together. In both of these tests, the specimens were subjected to in-plane loading only.

In the Phase 2-CG wall tested here, the sacrificial corner bead detached (DS 1) at low drifts, similar to slip-track detailing with typical intersection details. However, DS 2 and DS 3 were not observed until after 2% drift. By comparison, the CG detail tested in Retamales et al. (2013) never sustained DS 2 or DS 3 but was subjected only to in-plane loading. The Retamales et al. (2013)-DST detailing was successful in delaying DS 1 up to 1% story drift; however, the DS 2 and DS 3 occurred in the same drift range as typical slip-track detailing. In the Phase 2-DG wall evaluated here, expansion joints helped to delay DS 1 to about 1% story drift (Table 6). Only the expansion joints adjacent to the wall intersections were effective in reducing the damage. Also, Araya-Letelier's sliding/frictional connection was shown to successfully isolate the partition walls from any damage up to a displacement of 37 mm (drift = 1.5%). Damage occurred shortly after reaching the free sliding limit of 32 mm, which was determined by the size of the circular hole in the track. Jenkins et al. (2016) reported on additional experimental tests of the sliding/frictional connection incorporated in a building test-bed. Damage to the walls initiated at drifts less than 1% in these experiments, which is partially explained by the fact that the free sliding limit (constant at 32 mm) corresponded to a lower drift due to the increased story height. At larger drifts, Jenkins et al. (2016) reported damage characteristics similar to a fixed connection, such as dislodging of the screw head from the plaster coating and plastic hinging of studs. However, noticeable reductions in tape damage and cracks in the wall corners were observed.

In comparing the connections, the sliding/frictional connection (Araya-Letelier, Miranda, and Deierlein 2019) was most successful in delaying the onset of damage (DS 1), but this connection will be less effective for taller story heights. However, the range of drift percentages observed in DS 2 and DS 3 was comparable for the Phase 2-CG wall and the sliding/frictional connection. The Phase

2-DG wall was shown to be another possible approach to delay the initiation of damage; however, total damage (DS 3) occurred at only incrementally larger drifts.

Another study worth mentioning is Tasligedik, Pampanin, and Palermo (2013), but it was not included in Table 6 because the setup did not incorporate return walls. The study explored gap details similar in concept to the Phase 2-DG wall. First, gaps totaling 40 mm in width, which could accommodate 1.5% drift, were provided at the wall ends and between drywall panels. Second, the drywall was only connected to the studs, and the studs were friction fitted to allow for sliding. The partition walls were tested as an infill wall within a concrete frame. The performance of this detail was much better than the Phase 2-DG wall. However, the structural integrity of this detail might be challenged when implemented with typical return wall configurations rather than bound by a rigid frame, and fire protection remains an issue.

3.3. Influence of Rocking Wall Uplift on Partition Wall Response

In this test, the collector beam was connected to the CLT rocking wall by an eccentric round pin through a vertical slot at the wall. The intended behavior of the connection is that the collector beam and floor diaphragm do not uplift when the CLT wall rocks up off the foundation.

Figure 14 presents several measurements to quantify the impact of rocking wall uplift during the tests. For the Phase 1 walls at a drift cycle of 3.2%, Fig. 14(a) shows the uplift of the south wall at the location of the pin. Since the pin was located eccentrically on the rocking walls, the uplift was asymmetric. Figure 14(b) shows movement across the vertical gap at the top of the partition walls at various sensor locations (PSE 2, PSE3, PSW2, and PSW3 in Fig. 14(b)). Notably, the movement of the diaphragm was not sufficient to close the vertical gap of 9.5 (depicted as negative in Fig. 14(b)) or open the gap (depicted as positive in Fig. 14(b)) enough to cause the stud and track (overlapping by 41.3 mm) to pull apart. There was no real correlation between movement across the gap and proximity to the rocking wall, which suggests that these partition walls were not affected by localized diaphragm deformation.

Figure 14(c) is analogous to Fig. 14(a) for Phase 2 tests, except that the vertical displacements of the adjacent collector beam at the pin and near the column, which were only measured in Phase 2, are also shown. The relative movements across the partition wall vertical gap are shown in Fig. 14(d,Fig. 14(e)) at the main wall sensor locations (PSW4, PSW5, and PSE7) and return wall sensor locations (PSW1, PSW8, PSE1, and PSE10), respectively. The uplift was reduced significantly from the wall to the collector beam due to the introduction of the slotted connection (Fig. 14(c)). However, this connection did not completely prevent the vertical movement of the collector beam at higher drifts, probably due to increased friction as the wall rotated. The collector beam started to displace upward at about 2% drift, and its displacement was comparable to the wall uplift thereafter. The provided gap at the top of the partition wall was again sufficient to accommodate the movement of the diaphragm for Phase 2 walls, even though the main CG wall was in much closer proximity to the rocking wall. Moreover, the relative vertical movement across the partition walls gap was more significant for wall locations near the south end of the diaphragm (PSW4, PSW1, and PSE1) than at other locations. Larger vertical movements were believed to occur at these locations due to proximity to the collector beam or end of the diaphragm, and the corners being less restrained by gravity load.

Figure 15 shows the maximum and minimum value of vertical displacement/movement across the gap in the in-plane cycle of each stage. The maximum values correspond to the opening of the gap (Fig. 15(a)), and the minimum values correspond to the closing of the gap (Fig. 15(b)). As noted earlier, after 2% drift, a greater portion of the wall uplift transferred to the collector beam both near the column and at the pin location. Moreover, this vertical movement of the collector beam more significantly affected partition wall locations at the end of the diaphragm (south sensors), so these locations experienced a significant increase in the vertical movement across the gap after a 2% drift compare to other locations.
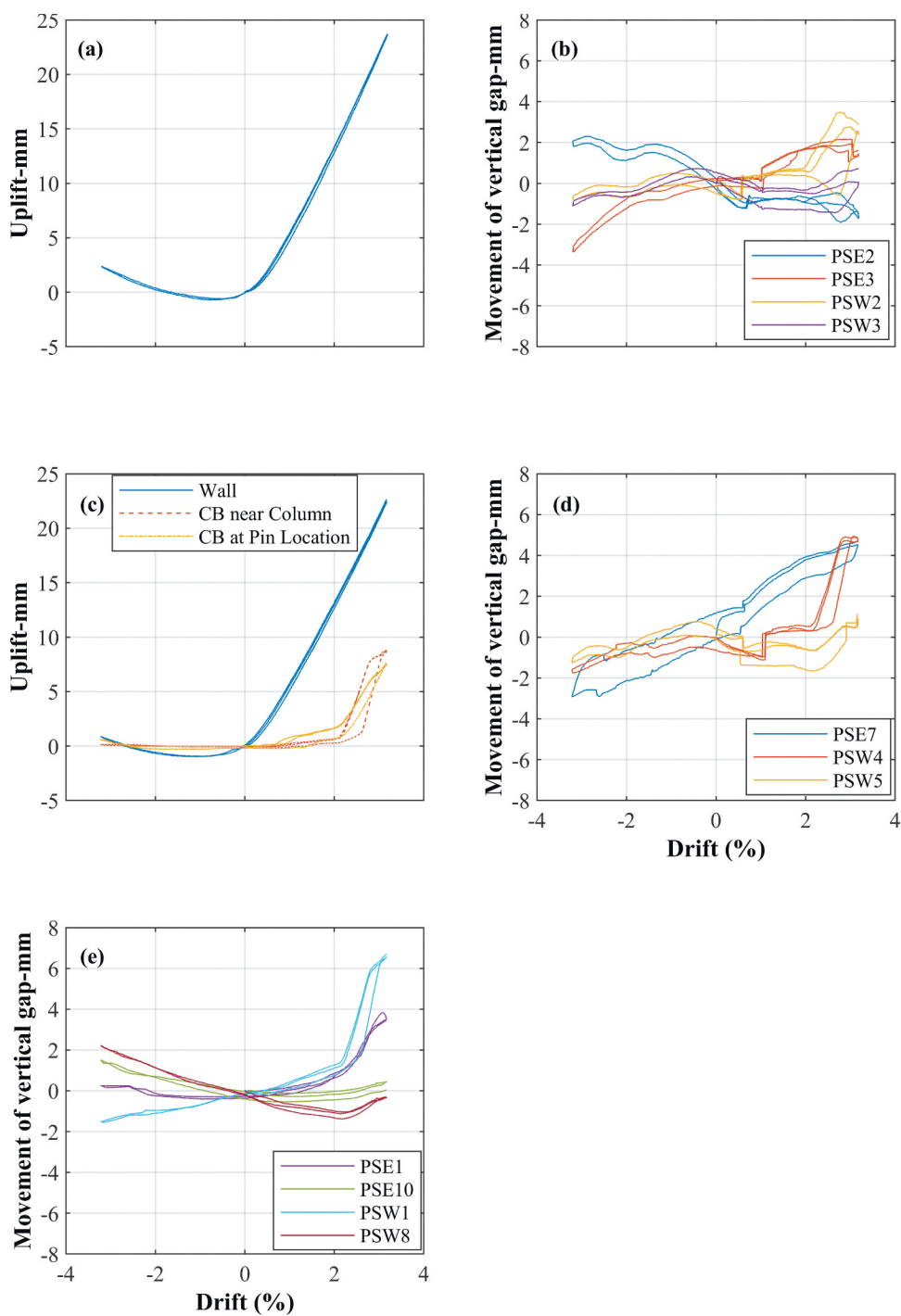
Figure 14. Phase 1: (a) uplift at the wall-pin location, (b) relative vertical movement of gaps at the top of partition walls; Phase 2: (c) uplift at the wall-pin location and vertical movement of collector beam, and relative vertical movement of gaps at the top of the (d) main walls, and (e) return walls.
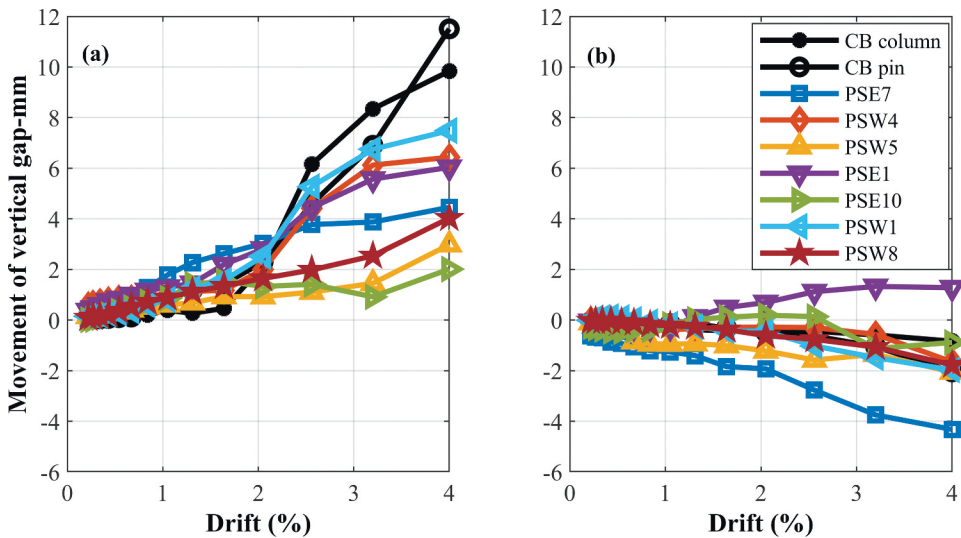
Figure 15. Movement of vertical gaps – positive values: opening – negative values: closing; (a) maximum value in a stage, (b) minimum value in a stage.

4. Conclusion

This paper has addressed concerns about demands imposed to non-structural components in buildings using the CLT rocking wall as a resilient lateral system, such as large inter-story drifts and diaphragm deflection due to the uplift of the rocking wall. Experiments of partition walls integrated into a CLT rocking wall subassembly subjected to quasi-static bidirectional loading were performed at the NHERI Lehigh EF. Different configurations of partition walls were selected to study the effect of different construction details for reducing the drift induced damage in the partition walls. Phase 1 focused on the seismic performance of partition walls detailed to slip/slide, wherein a telescoping detail was compared to a traditional slip-track connection detail in two straight walls. Phase 2 incorporated return walls and investigated details aimed at isolation/separation of intersecting walls to reduce impact. A CG detail and DG detail were incorporated into C-shaped walls to reduce the damage that occurs at the wall intersections. The major findings are summarized as follows:

- In Phase 1, the telescoping detailing proved to be more favourable than traditional slip track detailing, as it was observed to eliminate damage to the framing of partition walls caused by the separation of the end studs from the track at large drifts.
- In the Phase 2 DG wall, expansion joints helped to delay the onset of damage to about 1% story drift. Only the expansion joints adjacent to the wall intersections were effective in reducing the damage. However, the introduction of expansion joints on both walls adjacent to a corner is not recommended due to a potential stability issue at large drifts. As the joints on both walls opened, a small corner section of the wall detached from the rest and posed a local collapse risk.
- In the Phase 2 CG wall, the sacrificial corner bead detached at low drifts, but DS 2 and DS 3 occurred at much higher drifts compared to other C-shaped walls detailed without the CG. This approach has promise as a low damage detail and should be explored in additional configurations; however, it still needs evaluation of fire resistance and acoustic transmission.
- The contribution of partition walls to the lateral resistance may be significant in flexible mass timber construction. Based on the results, however, stiffness and strength of all wall details were negligible except the DG wall, which behaved like the traditional wall-intersection after the closure of the expansion joints. The strength of partition walls was insignificant compared to the whole subassembly in both phases.

- For all partition walls, out-of-plane drift did not affect the in-plane resistance, but some of the damage phenomena initiated specifically during the out-of-plane cycles and, as a result, at lower drifts than in comparable prior studies. For example, in contrast to previous studies, DS 3 was observed in the slip track wall without return walls due to damage to the track legs, which may have been caused by out-of-plane loading. Furthermore, in the CG wall, DS 2 and 3 were observed despite not having been observed in previous studies.
- Furthermore, providing a stud-track and gypsum-diaphragm gap is fundamental for accommodating the diaphragm deflection. However, the vertical movement of the diaphragm due to the influence of the rocking wall uplift was insignificant up to 2% drift, and after that, a portion of uplift transferred to the collector beam and the adjacent diaphragm. In general, the provided gap at the top of the partition walls was sufficient for accommodating this movement.
- Minimizing the damage that occurs at the corners of the partition walls has proven challenging. However, in the CG wall detail, damage to the framing was associated specifically with the slip-track detailing. The authors hypothesize that combining telescoping tracks and the CG detail will be the best option for reducing the damage at wall intersections. This configuration and others will be explored in an upcoming shake-table test on a ten-story CLT rocking wall building at NHERI@UCSD. Industry consultants will provide input to verify that these innovative details are constructible and satisfy fire rating and acoustic requirements.

ORCID

Hamed Hasani http://orcid.org/0000-0003-3018-1108
Keri L. Ryan http://orcid.org/0000-0002-0076-1630

References

Applied Technology Council. 2007. *Interim testing protocols for determining the seismic performance characteristics of structural and nonstructural components. -FEMA 461.*

Applied Technology Council. 2012. *Reducing the risks of nonstructural earthquake damage – a practical guide. - FEMA E-74.*

Araya-Letelier, G., and E. Miranda. 2012. "Novel sliding/frictional connections for improved seismic performance of gypsum wallboard partitions." In the *15th World Conference on Earthquake Engineering.* Lisbon, Portugal.

Araya-Letelier, G., E. Miranda, and G. Deierlein. 2019. "Development and testing of a friction/sliding connection to improve the seismic performance of gypsum partition walls.". *Earthquake Spectra* 35 (2): 653–77. doi: 10.1193/123117EQS270M.

ASCE (American Society of Civil Engineers). 2003. *ASCE/SEI 41-13: Seismic evaluation of existing buildings.* Reston, Virginia: American Society of Civil Engineers.

ASCE (American Society of Civil Engineers). 2007. *ASCE/SEI 41-06: Seismic rehabilitation of existing buildings.* Reston, Virginia: American Society of Civil Engineers.

Blume, J. A., Associates. 1966. *First progress report on racking tests of wall panels-report NVO-99-15*. San Francisco, CA: URS/John A. Blume & Associates Engineers.

Blume, J. A. Associates. 1968. *Second progress report on racking tests of wall panels-report NVO-99-35*. San Francisco, CA: URS/John A. Blume & Associates Engineers.

Bond, R., A. Amer, R. Sause, and J. Ricles 2018. *PRJ-2054: Undergraduate research experience (REU), NHERI 2018: Self-centering cross-laminated timber walls erection and instrumentation plan. DesignSafe-CI*, doi:10.17603/DS2GT2M

Buchanan, A., B. Deam, M. Fragiacomo, S. Pampanin, and A. Palermo. 2008. "Multi-storey prestressed timber buildings in New Zealand.". *Structural Engineering International* 18 (2): 166–73. doi: 10.2749/101686608784218635.

Clay, A., A. Amer, R. Sause, and J. Ricles. 2019. *PRJ-2487 undergraduate research experience (REU), NHERI 2019: Seismic tests of self-centering CLT shear wall with floor diaphragm and gravity load system. DesignSafe-CI*, doi: 10.17603/DS2NFDPXE86

Davies, R. D., R. Retamales, G. Mosqueda, and A. Filiatrault. 2011. *Experimental seismic evaluation, model parameterization, and effect of cold-formed steel-framed gypsum partition walls on the seismic performance of an essential facility-MCEER-11-0005*. New York: University at Buffalo, State University of New York.

FEMA. 2000. *Prestandard and commentary for the seismic rehabilitation of buildings (FEMA 356)*. Washington, DC: Federal Emergency Management Agency.

Fiorino, L., B. Bucciero, and R. Landolfo. 2019. Evaluation of seismic dynamic behaviour of drywall partitions, façades, and ceilings through shake table testing. *Engineering Structures* 180 (November 2018): 103–23. Elsevier. doi: 10.1016/j.engstruct.2018.11.028.

Fiorino, L., T. Pali, B. Bucciero, V. Macillo, M. T. Terracciano, and R. Landolfo. 2017. Experimental study on screwed connections for sheathed CFS structures with gypsum or cement based panels. *Thin-Walled Structures* 116 (January): 234–49. doi: 10.1016/j.tws.2017.03.031.

Fiorino, L., T. Pali, and R. Landolfo. 2018. "Out-of-plane seismic design by testing of non-structural lightweight steel drywall partition walls.". *Thin-Walled Structures* 13: 213–30. doi: 10.1016/j.tws.2018.03.032..

Freeman, S. A. 1971. *Third progress report on racking tests of wall panels-report (JAB-99-54)*. California, U.S.A: San Francisco.

Freeman, S. A. 1974. *Fourth progress report on racking tests of wall panels-report (JAB-99-55)*. California, U.S.A: San Francisco.

Freeman, S. A. 1976. "Racking tests of high-rise building partitions." *Journal of the Structural Division* 103 (8): 1673–85.

Ganey, R. S. 2015. "Seismic design and testing of rocking cross laminated timber walls." The University of Washington.

Hasani, H., K. L. Ryan, A. Amer, J. M. Ricles, and R. Sause. 2018. "Pre-test seismic evaluation of drywall partition walls integrated with a timber rocking wall." In *Proceeding of the US National Conference on Earthquake Engineering*. Los Angeles, California, 11. doi:10.1002/eqe.

International Building Code Council. 2011. *2012International building code (IBC)*. Country Club Hills, IL: ICC.

Jenkins, C., S. Soroushian, E. Rahmanishamsi, and E. Manos Maragakis. 2016. Experimental fragility analysis of cold-formed steel-framed partition wall systems. *Thin-Walled Structures* Elsevier: 103: 115–27. doi: 10.1016/j.tws.2016.02.015.

Lee, T.-H., M. Kato, T. Matsumiya, K. Suita, and M. Nakashima. 2007. Seismic performance evaluation of non-structural components: Drywall partitions. *Earthquake Engineering & Structural Dynamics* 36 (3): 367–82. doi: 10.1002/eqe.638.

Magliulo, G., C. Petrone, V. Capozzi, G. Maddaloni, P. Lopez, and G. Manfredi. 2014. Seismic performance evaluation of plasterboard partitions via shake table tests. *Bulletin of Earthquake Engineering* 12 (4): 1657–77. doi: 10.1007/s10518-013-9567-8.

Matsuoka, Y., K. Suita, S. Yamada, Y. Shimada, and M. Akazawa. 2008. "Non-structural component performance in 4-story frame tested to collapse." In *Proceeding of the 14th World Conference on Earthquake Engineering*, 8. Beijing, China.

McCormick, J., Y. Matsuoka, P. Pan, and M. Nakashima. 2008. "Evaluation of non-structural partition walls and suspended ceiling systems through a shake table study." In *Proceedings of the 2008 Structures Congress - Structures Congress 2008: Crossing the Borders,* Vanvouver, BC, Canada, 314. doi:10.1061/41016(314)223.

Memari, A. M., B. Kasal, H. B. Manbeck, and A. R. Adams. 2008. "Experimental cyclic racking evaluation of light-frame wood stud and steel stud wall systems," *PHRC Research Series Rep, 107*.

Moroder, D., F. Sarti, A. Palermo, S. Pampanin, and A. H. Buchanan. 2014. "Experimental investigation of wall-to-floor connections in post-tensioned timber buildings." *NZSEE Conference*, Auckland (pp 21–23).

Mosqueda, G. 2016. *Interior cold-formed steel framed gypsum partition walls. - Background Document FEMA P-58/BD-3.9.32*.

"NHERI TallWood Research Tasks." 2020. Accessed April 21, 2020. http://nheritallwood.mines.edu/task3.html

"NHERI TallWood-Home." 2020. Accessed April 13, 2020. http://nheritallwood.mines.edu/.

Pali, T., V. Macillo, M. T. Terracciano, B. Bucciero, L. Fiorino, and R. Landolfo. 2018. In-plane Quasi-static cyclic tests of nonstructural lightweight steel drywall partitions for seismic performance evaluation. *Earthquake Engineering & Structural Dynamics* 47 (6): 1566–88. doi: 10.1002/eqe.3031.

Peck, Q., N. Rogers, and R. Serrette. 2012. "Cold-formed steel framed gypsum shear walls: In-Plane response." *Journal of Structural Engineering* 138 (7): 932–41. doi: 10.1061/(ASCE)ST.1943-541X.0000521.

Pei, S., J. W. van de Lindt, A. R. Barbosa, J. W. Berman, E. Mcdonnell, J. Daniel Dolan, H.-E. Blomgren, R. B. Zimmerman, D. Huang, S. Wichman, et al. 2019. Experimental seismic response of a resilient 2-story mass-timber building with post-tensioned rocking walls. *Journal of Structural Engineering* 145 (11): 04019120. doi: 10.1061/(ASCE)ST.1943-541X.0002382.

Petrone, C., G. Magliulo, P. Lopez, and G. Manfredi. 2015. Seismic fragility of plasterboard partitions via In-Plane Quasi-static tests. *Earthquake Engineering & Structural Dynamics* 44 (14): 2589–606. doi: 10.1002/eqe.2600.

Petrone, C., G. Magliulo, P. Lopez, and G. Manfredi. 2016. Out-of-Plane seismic performance of plasterboard partition walls via Quasi-Static. *Bulletin of the New Zealand Society for Earthquake Engineering* 49 (1): 125–37. doi: 10.5459/bnzsee.49.1.125-137.

Rahmanishamsi, E., S. Soroushian, and E. M. Maragakis. 2016a. Evaluation of the Out-of-Plane behavior of stud-to-track connections in nonstructural partition walls. *Thin-Walled Structures* Elsevier: 103: 211–24. doi: 10.1016/j.tws.2016.02.018.

Rahmanishamsi, E., S. Soroushian, and M. Maragakis. 2016b. Cyclic shear behavior of gypsum board-to-steel stud screw connections in nonstructural walls. *Earthquake Spectra* 32 (1): 415–39. doi: 10.1193/062714EQS091M.

Restrepo, J. I., and A. F. Lang. 2011. Study of loading protocols in light-gauge stud partition walls. *Earthquake Spectra* 27 (4): 1169–85. doi: 10.1193/1.3651608.

Restrepo, J. I., and A. M. Bersofsky. 2011. Performance characteristics of light gage steel stud partition walls. *Thin-Walled Structures* 49 (2): 317–24. doi: 10.1016/j.tws.2010.10.001.

Retamales, R., G. Mosqueda, A. Filiatrault, and A. Reinhorn. 2011. Testing protocol for experimental seismic qualification of distributed nonstructural systems." *Earthquake Spectra* 27 (3): 835–56. doi: 10.1193/1.3609868.

Retamales, R., R. Davies, G. Mosqueda, and A. Filiatrault. 2013. Experimental seismic fragility of cold-formed steel framed gypsum partition walls. *Journal of Structural Journal of Structural Engineering* 139 (August): 1285–93. doi: 10.1061/(ASCE)ST.1943-541X.0000657.

Rihal, S. S. 1982. Behavior of non-structural building partitions during earthquakes. *Proceeding of the Seventh Symposium on Earthquake Engineering* 1: 267–77. University of Roorkee

Ryan, R., and Hasani, H. 2020. "Experimental Seismic Test of Drywall Partition Walls with Improved Detailing for Damage Reduction." 17th World Conference on Earthquake Engineering, 17WCEE, Sendai, Japan, 1–11.

Schoettler, M. J., A. Belleri, D. Zhang, J. I. Restrepo, and R. B. Fleischman. 2009. Preliminary results of the shake-table testing for the development of a diaphragm seismic design methodology. *PCI Journal* 54: 100–24. doi: 10.15554/pcij.01012009.100.124.

Soroushian, S., E. Manos Maragakis, K. L. Ryan, E. Sato, T. Sasaki, T. Okazaki, G. Mosqueda. 2016. Seismic simulation of an integrated ceiling-partition wall-piping system at E-Defense. II: Evaluation of nonstructural damage and fragilities. *Journal of Structural Engineering* 142 (2): 1–17. doi: 10.1061/(ASCE)ST.1943-541X.0001385.

Soroushian, S., K. L. Ryan, M. Maragakis, J. Wieser, T. Sasaki, E. Sato, T. Okazaki, et al. 2012. "NEES/E-defense tests: Seismic performance of ceiling/sprinkler piping nonstructural systems in base isolated and fixed base building." *15th World Conference on Earthquake Engineering.* (15WCEE), Lisbon, Portugal.

SSMA (Steel Stud Manufacturers Association). 2000a. "Single deflection track selection." 2000.

SSMA (Steel Stud Manufacturers Association). 2000b. "Track within a track deflection assembly." 2000.

Swensen, S., G. G. Deierlein, and E. Miranda. 2015. Behavior of screw and adhesive connections to gypsum wallboard in wood and cold-formed steel-framed wallettes. *Journal of Structural Engineering* 142 (4). doi: 10.1061/(ASCE)ST.1943-541X.0001307.

Taghavi, S., and E. Miranda. 2003. "Response assessment of nonstructural building elements." *Report PEER 2003/05, Pacific Earthquake Engineering Research Center*, University of California, Berkeley, 96.

Tasligedik, A. S., S. Pampanin, and A. Palermo. 2012. "In-Plane cyclic testing of non-structural drywalls infilled within RC frames In The *15th World Conference on Earthquake Engineering (15WCEE)*. Lisbon, Portugal.

Tasligedik, A. S., S. Pampanin, and A. Palermo. 2013. "Low damage seismic solutions for non-structural drywall partitions." In The *Vienna Congress on Recent Advances in Earthquake Engineering and Structural Dynamics (VEESD 2013)*, 11. Vienna, Austria. doi:10.1007/s10518-014-9654-5.

Villaverde, R. 1997. Seismic design of secondary structures: State of the art. *Journal of Structural Engineering* 123 (August): 1011–19. doi: 10.1061/(ASCE)0733-9445(1997)123:8(1011).

Wang, X., T. C. Elide Pantoli, J. I. Hutchinson, R. L. Restrepo, M. S. Wood, P. G. Hoehler, F. H. Sesma, and F. H. Sesma. 2015. Seismic performance of cold-formed steel wall systems in a full-scale building. *Journal of Structural Engineering* 141 (10): 1–11. doi: 10.1061/(ASCE)ST.1943-541X.0001245.

Zhou, Y., R. Li, and X. L. Lu. 2012. "Earthquake-resilient tall buildings using rocking walls." In The *15th World Conference on Earthquake Engineering*, Lisbon, Portugal.